Interfacial spin-glass-like state in Mn_5Ge_3 single crystalline films grown on germanium substrates

A. Truong,[1] A. O. Watanabe,[1] P. A. Mortemousque,[1] K. Ando,[1] T. Sato,[2] T. Taniyama,[3] and K. M. Itoh[1,*]

[1]*School of Fundamental Science and Technology, Keio University, 3-14-1 Hiyoshi, Kohoku-ku, Yokohama 223-8522, Japan*

[2]*School of Integrated Design Engineering, Keio University, 3-14-1 Hiyoshi, Kohoku-ku, Yokohama 223-8522, Japan*

[3]*Materials and Structures Laboratory, Tokyo Institute of Technology, 4259 Nagatsuta, Midori-ku, Yokohama 226-8503, Japan*

(Received 4 May 2015; revised manuscript received 4 June 2015; published 22 June 2015)

Thermal irreversibility of the magnetization in Mn_5Ge_3 epitaxial thin films on Ge(111) is reported. The frequency dependence of the ac susceptibility demonstrates a spin-glass-like behavior, despite the fact that the thin film is a single crystal. Such glassy behavior is attributed to the presence of a "ferromagnetically dead" layer with spin-glass-like properties at the Mn_5Ge_3/Ge interface, which results in frustrated interactions with the ferromagnetic Mn_5Ge_3. Moreover, it is shown that the magnetic phase diagram in the H-T plane of the glassy state is very sensitive to the growth conditions. Variation in the growth temperature and film thickness changes the spin-glass-like properties and the Curie temperature. The sensitivity of the glassy state to the growth conditions is related to the variation in the properties of the interfacial layer.

DOI: 10.1103/PhysRevB.91.214425 PACS number(s): 75.70.Ak, 75.50.Lk, 75.30.Cr, 37.20.+j

I. INTRODUCTION

The spin-glass phase is one of the most complex systems in solid-state physics for it lacks the long-range order due to the competitive interactions between randomly distributed spins [1]. Contrary to the ferromagnetic and paramagnetic phases, the spin-glass state is nonergodic. A noticeable feature of such a system is a spin-freezing process arising from the slow magnetization dynamics. Recently, the emergence of exchange bias was reported for spin-glass/ferromagnet hybrid systems [2,3]. The exchange bias in spin glasses can lead to the unique property of inverted bias effect [3,4], which causes the exchange bias field to change its sign for a temperature range below the blocking temperature. Interactions of spin currents with spin glasses are also investigated actively [5]. Such phenomena are expected to play important roles in the wide range of future spintronics applications. One of the routes to form nanoscale spin-glass/ferromagnet systems is making use of the so-called naturally formed spin-glass layers. Recent studies have shown that a spin-glass behavior can arise at the surface or interface of a magnetically ordered phase, due to a surface effect or a translational symmetry breaking of the lattice [6–10]. This leads to spin frustration and competing magnetic interactions in the ordered phase. The understanding of such competing interactions at the surface or interface is of great importance because it can significantly alter the properties of magnetic thin films.

The Mn_5Ge_3 ferromagnetic compound has been attracting much attention since single crystalline Mn_5Ge_3 films that have Curie temperatures of about 295 K can be grown epitaxially on Ge(111) by solid phase epitaxy [11–16]. High spin injection efficiency is expected from Mn_5Ge_3 to Ge substrates [17]. In this paper, we demonstrate that Mn_5Ge_3 in the form of a thin film on Ge(111) does not show simple ferromagnetism in the entire range of temperature below its Curie point. The zero-field-cooling (ZFC) and field-cooling (FC) curves indicate the presence of a thermal irreversibility in the magnetization. The characterization of the ac susceptibility leads to the conclusion that the nature of the irreversibility is similar to that of a spin glass, despite the fact that no apparent signs of disorder or frustration can be found in such single crystalline thin films. The spin-glass-like behavior is attributed to the presence of a "ferromagnetically dead" layer at the Mn_5Ge_3/Ge interface. Indeed, thickness dependence of the ferromagnetism in Mn_5Ge_3/Ge(111) has shown that a thickness of approximately 1.7 nm of the thin film from the Mn_5Ge_3/Ge interface does not contribute to the total magnetic moment [18]. However, no magnetic characterization of such "ferromagnetically dead" layer was performed in the past. This work shows that the spin-glass nature attributed to the "dead" layer explains the frustrated interactions observed in the ferromagnetic part of the film. It is also shown that the temperature dependence of the stability of the spin-glass-like state in a magnetic field follows the de Almeida-Thouless line. Section II describes the experimental techniques and structural characterizations. Section III provides thorough experimental characterizations of the glassy state in Mn_5Ge_3 on Ge(111). Finally, Sec. IV discusses the influence of the growth conditions on the thermal irreversibility of the magnetization.

II. EXPERIMENTAL DETAILS

The Mn_5Ge_3 thin films were grown on Ge(111) substrates by solid phase epitaxy in a molecular beam epitaxy chamber, in which the base pressure was less than 10^{-8} Pa. Three kinds of samples were studied in this work as presented in Table I. For each sample, a thin layer of Mn was deposited on a $c(2 \times 8)$ reconstructed Ge surface. A solid-state reaction between the Ge single crystal and the deposited Mn was induced by annealing the samples at 150 °C (samples A and C) or 200 °C (sample B) leading to the solid-state growth of single crystalline Mn_5Ge_3 thin films. The annealing process yielded the well-established $\sqrt{3} \times \sqrt{3}$ structure of the $Mn_5Ge_3(001)$ surface, as can be seen from the reflection high-energy electron diffraction (RHEED) patterns in Fig. 1(a). $Mn_5Ge_3(001)$ grew coherently on Ge(111) due to the fact that the in-plane atomic distance in the [010] direction of the hexagonal Mn_5Ge_3 ($d_{Mn_5Ge_3} = 7.112$ Å) was relatively close

*kitoh@appi.keio.ac.jp

TABLE I. List of the samples studied in this work. T_{SPE} is the growth temperature and refers to the annealing temperature used for the solid phase epitaxy of Mn_5Ge_3. The final thickness of the Mn_5Ge_3 layer is $t_{Mn_5Ge_3}$. The variation of the Curie temperature T_C will be discussed in Sec. IV.

Name	Deposited Mn (nm)	T_{SPE} (°C)	$t_{Mn_5Ge_3}$ (nm)	T_C (K)
Sample A	∼11.4	150	∼17	294
Sample B	∼11.4	200	∼17	290
Sample C	∼22.8	150	∼33	288

to the in-plane atomic distance in the $[11\bar{2}]$ direction of the cubic Ge substrate ($d_{Ge} = 6.937$ Å). Here, the lattice mismatch is only about 2.4% [19]. An amorphous Ge capping layer was grown to prevent the oxidization of the magnetic layer. Transmission electron microscopy (TEM) was employed to confirm the epitaxial growth of Mn_5Ge_3 on the Ge single crystal and the absence of clusters of other stoichiometries in either layers [see Fig. 1(b)]. The x-ray diffraction (XRD) patterns shown in Fig. 1(c) confirmed the epitaxial relationship $Mn_5Ge_3(001)/Ge(111)$ and did not detect the presence of phases other than Mn_5Ge_3. The in-plane distances $d_{Mn_5Ge_3}$ and d_{Ge} were evaluated from off-normal angle XRD measurements (not shown here).

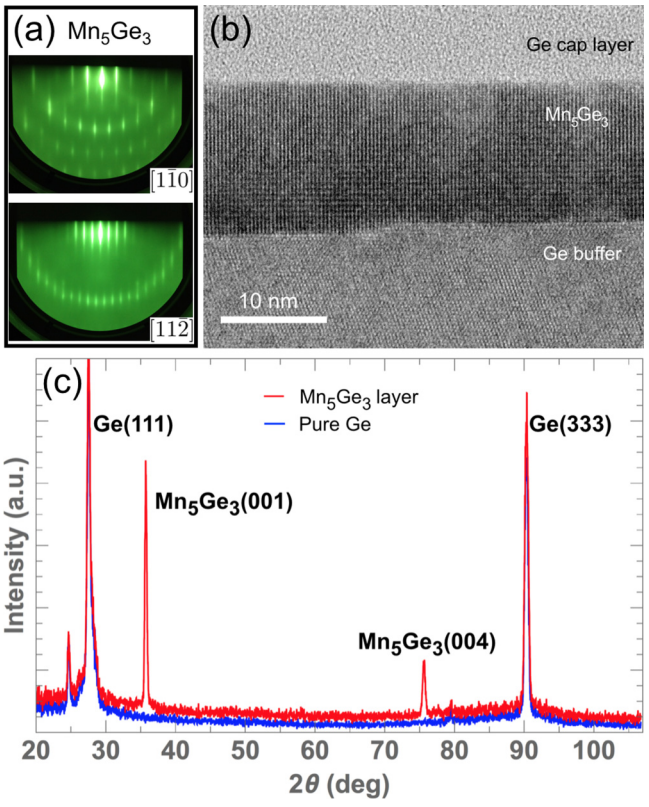

FIG. 1. (Color online) (a) RHEED patterns of the $\sqrt{3} \times \sqrt{3}$ structure of Mn_5Ge_3 in the $[1\bar{1}0]$ and $[11\bar{2}]$ directions of the Ge substrate. (b) The cross-sectional TEM image of $Mn_5Ge_3(001)$ on Ge(111). (c) An XRD pattern of the Mn_5Ge_3 layer (red curve) and a pure Ge sample (blue curve) measured using Cu $K\alpha$ radiation. The peak at $2\theta = 24.6°$ is the signal from Ge under Cu $K\beta$ radiation originating from the x-ray source.

The magnetic properties of the samples were measured by a superconducting quantum interference device (SQUID) magnetometer. Due to the high sensitivity of the Mn_5Ge_3 thin films to the negative fields trapped in the superconducting magnet of the SQUID [20], the residual fields were removed by using a fluxgate magnetometer in a magnetic shield of permalloy in order to perform ultra-low-field measurements.

III. CHARACTERIZATION OF THE THERMAL IRREVERSIBILITY OF THE MAGNETIZATION

A. Zero-field- and field-cooled magnetization curves

This section explores the temperature dependencies of the magnetization of sample A. The properties of samples B and C will be discussed in Sec. IV. The magnetic hysteresis curves of Mn_5Ge_3/Ge undergo a change in squareness depending on the temperature [21]. In the vicinity of the Curie temperature [Fig. 2(a)], the magnetization switching is mainly driven by irreversible domain-wall motion. However, at lower temperatures, the magnetization process is driven by coherent rotation [see Fig. 2(b)]. The remanence ratio is close to unity near the Curie point, but decreases and stabilizes at a lower value ($M_R/M_S \simeq 0.50$) below 200 K. The strong variation in remanence ratio between 290 and 200 K suggests for a sudden change in the in-plane magnetic anisotropy or in the exchange interaction [22]. However, the sample orientation dependence of the ferromagnetic resonance spectroscopy in our recent work [21] detected no in-plane magnetic anisotropy in the Mn_5Ge_3 thin films.

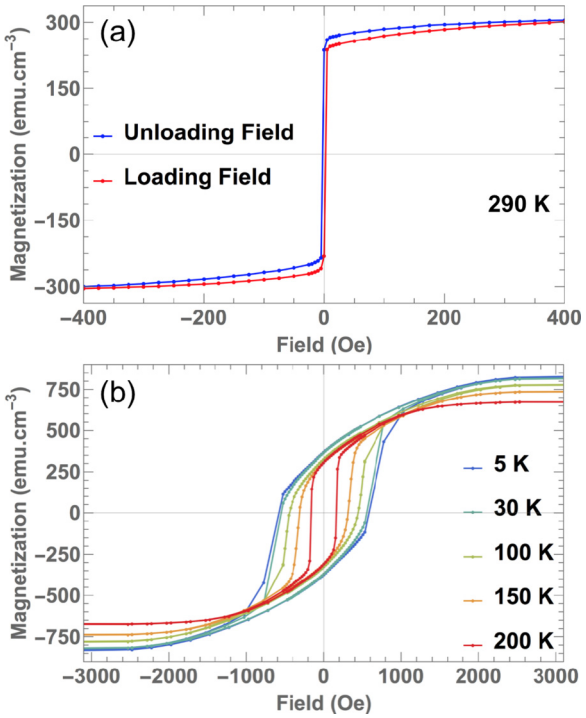

FIG. 2. (Color online) Hysteresis curves measured at temperatures (a) close to the Curie temperature and (b) from 5 to 200 K. In the vicinity of the Curie point, the coercivity is low and the remanence ratio is high, while it becomes opposite at lower temperatures.

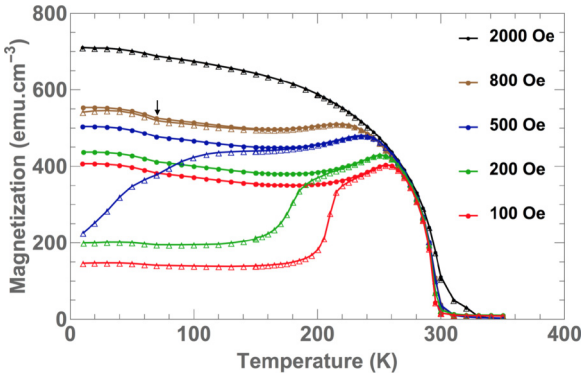

FIG. 3. (Color online) Zero-field-cooling and field-cooling curves for different values of dc magnetic field. The open symbols are for ZFC curves and filled symbols are for FC curves. Note the presence of kinks at about 65 K for each FC curve (marked by the arrow only for 800 Oe).

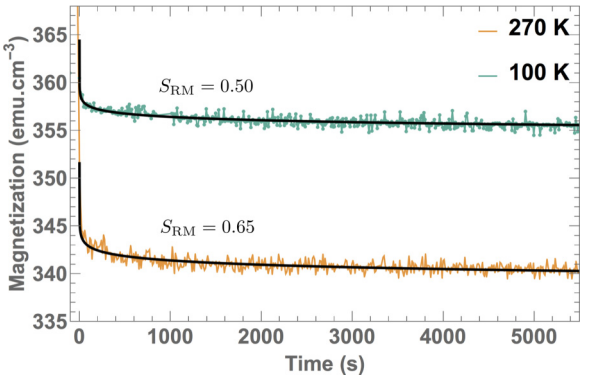

FIG. 4. (Color online) Time dependence of the TRM at 100 and 270 K. The black lines are fits using the logarithm law given in Eq. (1).

The temperature dependence of the magnetization measured under the ZFC and FC conditions is shown in Fig. 3. The ZFC and FC curves were measured by warming the sample from 10 to 350 K after cooling it from room temperature at zero and finite constant field, respectively. A thermal irreversibility clearly appears for fields below 2000 Oe, as evidenced by the nonzero difference between the FC and ZFC magnetizations. For each field, the presence of a Hopkinson maximum [23–25] is observed. The FC curves do not vary monotonously; they initially decrease with temperature and increase before reaching the maximum and finally decrease again once the maximum is passed, due to the transition to the paramagnetic phase. This behavior is related to the increase of magnetic domain wall mobility at low magnetic fields upon heating, thus leading to an increase in the ZFC magnetization activated by the thermal process. The results in Fig. 3 indicate that the interactions between spins become nonhomogeneous below a certain temperature depending on the applied field. Moreover, one can notice a kink in the magnetization at about 65 K for each FC curve as marked by an arrow in Fig. 3. The position of this sudden increase in magnetization for decreasing temperature seems not to be field dependent, although the effect becomes weaker at higher fields. Its physical meaning will be discussed later. The thermal irreversibility in the ZFC and FC magnetizations shows that the ferromagnetic order in epitaxial Mn_5Ge_3 on Ge(111) is affected by some glassy behavior.

In order to confirm the glassy behavior, the thermoremanent magnetization (TRM) was measured by cooling down from the paramagnetic state to a measurement temperature T_m, in the field-cooling condition under the field of 800 Oe. Here, when T_m was reached, the applied dc field was turned off and the magnetization was measured as a function of time. We have chosen two T_m, 100 and 270 K, to test the glassiness of the system. The reference time corresponded to the time at which the magnetic field was removed. The decays of the thermoremanent magnetization for the two T_m are best fitted with a logarithm function for the laboratory time scale, as seen in Fig. 4, by using the following relation:

$$M(t) = M_0 - S_{RM} \ln(t), \quad (1)$$

where M_0 is a constant and S_{RM} is the temperature-dependent magnetic viscosity [1]. Although successfully employed for some spin-glass systems [26–29], a stretched exponential function does not give any satisfactory fits in this case. The magnetic viscosity in the time dependence of the magnetization shown in Fig. 4 corresponds to the time lag between the changes in magnetization in response to the changes in the applied field. It occurs when energy barriers need to be overcome for the magnetization to decrease when the field is removed. Such slow decay of the TRM is consistent with a spin-glass-like behavior, for which the energy barriers are randomly distributed [29–32].

B. ac susceptibility of Mn_5Ge_3

The ac susceptibility of the Mn_5Ge_3 thin films was measured by applying a driving field $H(t) = H_{ac}\cos(\omega t)$, where H_{ac} and $\omega/2\pi$ are the driving amplitude and driving frequency, respectively. Measurements of the real (χ') and imaginary (χ'') parts of the susceptibility were performed with and without the bias dc field in the zero-field-cooling condition. The measurement at zero dc field in Fig. 5(a) clearly shows a divergent peak in the real part of the susceptibility at about 294 K. This temperature is consistent with the Curie point, therefore the peak matches with the paramagnetic (PM) to ferromagnetic (FM) transition. In addition to the sharp and intense peak at 294 K, a broad peak with less amplitude, whose maximum is located at about 275 K, is also observed. The presence of the maximum in the imaginary part at a temperature slightly lower than that of the real part indicates the presence of a relaxation process. Interestingly, the imaginary part of the ac susceptibility at zero dc field is of the same order of magnitude as that of the real part, and actually is larger in the absolute value. To our knowledge, no previous work reported the contribution of the out-of-phase term being higher than that of the in-phase term. The imaginary part represents the magnetic loss or irreversible process induced by absorption of energy from the ac magnetic field. In the present case, some unusual energy dissipation may be occurring at the irreversibility point. In the Mn_5Ge_3 thin film, both real and imaginary parts are sensitive to the presence of a superimposed dc field that is as small as 2 Oe [see Fig. 5(b)]. Due to the bias dc field, the intensity of the peak of the PM to FM transition

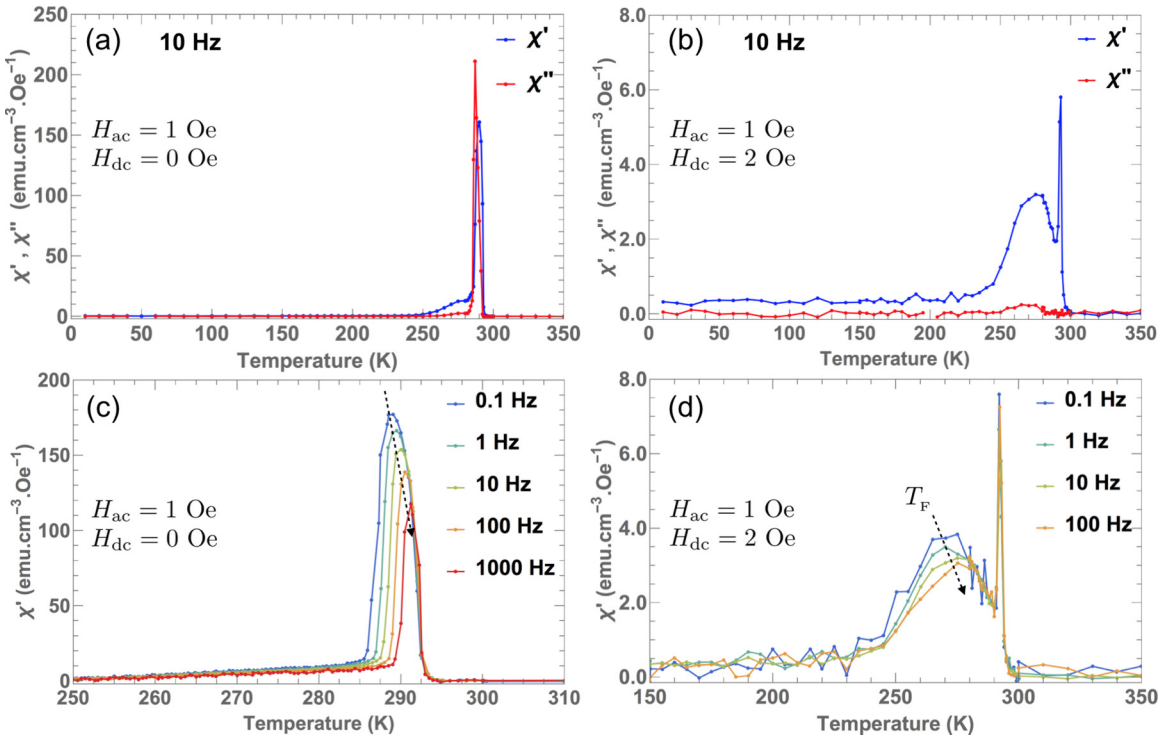

FIG. 5. (Color online) ac susceptibility measurements using the driving field of 1 Oe with no dc field [(a) and (c)] and with superimposed dc field of 2 Oe [(b) and (d)]. A driving frequency of 10 Hz was used in (a) and (b), for which both real and imaginary parts are shown. The frequency dependence of the real part χ' is shown with (c) zero dc field and (d) with a dc field of 2 Oe. The shifts in maximum of χ' with the increasing frequencies are indicated by dashed arrows.

substantially decreases, and what was seen as a small broad peak in Fig. 5(a) appears as a distinct feature in Fig. 5(b). The imaginary part of the susceptibility in Fig. 5(b) is reduced to one order of magnitude smaller than that of the real part. The maximum of the secondary peak in the real part of the susceptibility is slightly shifted to lower temperature (∼265 K) in the presence of the static field. This observation is consistent with the fact that the irreversibility temperature decreases with increasing fields (see Fig. 3). In Figs. 5(c) and 5(d), it is evidenced that the ac susceptibility is dependent on the frequency of the driving field, which is a sign of slowing down in the magnetization dynamics. In Fig. 5(d), the peak at 294 K is independent on frequency, which is expected for a transition to a long-range-ordered phase (PM to FM). On the other hand, the maximum of the secondary peak shifts towards higher temperatures with increasing frequencies, which is a common feature seen in spin glasses [33]. In summary, the results in Fig. 5 suggest that when the Mn_5Ge_3 thin film is cooled down from room temperature, it undergoes the PM to FM transition at 294 K. Further decrease in temperature leads to a slow magnetization dynamics occurring in the immediate vicinity of T_C at low fields.

The scaling laws are employed in order to quantify the frequency dependence of the spin-glass transition temperature T_F. Here, the shift in the spin-glass transition temperature (δT_F) per decade of frequency is given by

$$\delta T_F = \frac{\Delta T_F}{T_F \Delta[\log_{10}(\omega/2\pi)]}. \quad (2)$$

From Fig. 5(d), we estimate $\delta T_F \simeq 0.005$. Previous reports stated that δT_F usually ranged from 0.0045 to 0.06 for canonical spin glasses (e.g., CuMn), and $\delta T_F \geqslant 0.1$ for systems with noninteracting clusters, such as superparamagnets [33–37]. Consequently, the value of δT_F expected for our system is of the same order of magnitude as that of a canonical spin glass.

The hypothesis on the spin-glass-like behavior in our system is further supported by the fit of the frequency dependence of the susceptibility maxima using the critical exponent law

$$\tau = \tau_0^{\text{crit}} \left(\frac{T_F - T_{SG}}{T_F} \right)^{-z\nu}, \quad (3)$$

where $1/\tau = \omega/2\pi$ is the driving frequency, τ_0^{crit} is the characteristic relaxation time for a single spin flip, T_{SG} is the spin-glass transition temperature at zero frequency, and $z\nu$ is the dynamical exponent. Figure 6(a) shows a log-log plot corresponding to Eq. (3). The best fit is obtained with $z\nu \simeq 6.5$, $1/\tau_0^{\text{crit}} \simeq 1.1 \times 10^{12}$ Hz, and $T_{SG} = 266.5$ K. $z\nu \simeq 6.5$ is in the typical range found for spin glasses (between 4 and 12) [35,36,38] and $1/\tau_0^{\text{crit}} \simeq 1.1 \times 10^{12}$ Hz is compatible with the characteristic frequency reported for spin glasses ($10^8 \leqslant 1/\tau_0^{\text{crit}} \leqslant 10^{12}$ Hz) [35,38,39]. The Arrhenius law for the frequency dependence of the maximum of the ac susceptibility $1/\tau = 1/\tau_0 \exp(-E_a/k_B T_F)$ accounts for the time scale to overcome energy barriers by the activation process. However, this assumption does not work for our sample because it results in the unphysical values of $1/\tau_0 \sim 10^{193}$ Hz and the activation energy term $E_a/k_B = 1.2 \times 10^5$ K. (E_a and

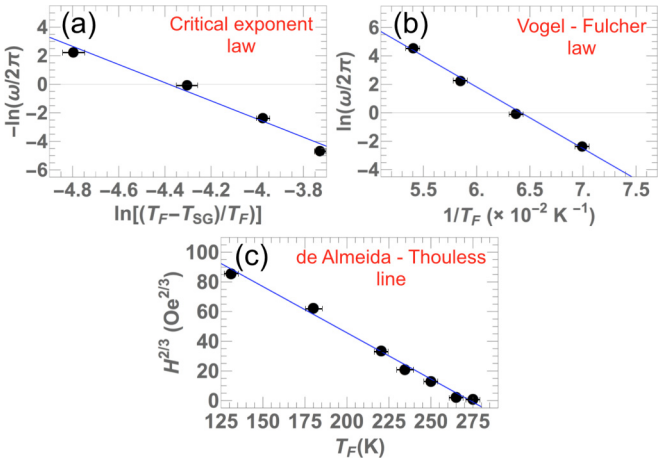

FIG. 6. (Color online) (a) Log-log plot of the critical exponent law for the frequency dependence of the spin-glass transition temperature, (b) Vogel-Fucher law, both fitted by using the data in Fig. 5(d). (c) $H^{2/3}$ as a function of T_F. The irreversibility temperatures are obtained from the ZFC and FC curves, by calculating the difference between the FC and ZFC magnetizations and determining the onset of nonzero difference.

k_B are the activation energy and the Boltzmann constant, respectively.) This invalidity of the Arrhenius law is consistent with the fact that the epitaxial Mn_5Ge_3 thin film does not contain any noninteracting magnetic clusters [34]. In order to take into account that the spins in the glassy state are interacting with each other and obtain the estimation of the activation energy, we employ the following phenomenological Vogel-Fulcher law:

$$\frac{1}{\tau} = \frac{1}{\tau_0} \exp\left[\frac{-E_a}{k_B(T_F - T_0)}\right], \tag{4}$$

where τ_0 has the same physical meaning as τ_0^{crit}, and T_0 is the empirical Vogel-Fulcher temperature, often interpreted as being related to the strength of the exchange interaction in the material [35,39–42]. The best fit, shown in Fig. 6(b), is obtained with $1/\tau_0 \simeq 1.2 \times 10^{12}$ Hz, which is consistent with the value found by the critical exponent law [Eq. (3)] and the activation energy of $E_a/k_B \simeq 433.2$ K. The Vogel-Fulcher temperature is determined to be $T_0 \simeq 254.3$ K. This relatively high value of the Vogel-Fulcher temperature suggests that the exchange interaction in the glassy state in the Mn_5Ge_3/Ge(111) heterostructure is stronger than $T_0 < 100$ K of other spin glasses reported in the literature [33,34,37]. The relationship between the Vogel-Fulcher law and the critical exponent was established in Ref. [39]. Here, one can find the dynamical exponent using the activation energy

$$\ln\left(\frac{40k_BT_F}{E_a}\right) \sim \frac{25}{z\nu}. \tag{5}$$

This relation gives $z\nu \simeq 7$, which is close to 6.5 obtained directly by the critical exponent analysis.

The dependence of the onset of irreversibility on the applied dc field is calculated using the onset of nonzero difference between the FC and ZFC magnetizations. The ac susceptibility vanishes at fields as small as a few Oe, thus making it difficult to probe the properties at higher fields. For Ising spin glasses, the mean-field theory predicts the existence of a transition line in the H-T plane referred to as the de Almeida-Thouless (AT) line [43–46]. The AT relation is derived from the Sherrington-Kirkpatrick theory describing the free energy of spin glasses [47]. The field dependence of the onset of irreversibility [9,47,48] can be analytically written as

$$\frac{H_{AT}}{\Delta J} \propto \left[1 - \frac{T_F}{T_F(H=0)}\right]^{3/2}, \tag{6}$$

where ΔJ is the width of distribution of exchange energy interaction and $T_F(H=0)$ is the glass transition temperature at zero field. A reasonable fit with the theoretical AT line is found for our material and gives a zero-field spin-glass-like transition temperature $T_F(H=0) \simeq 275$ K, as can be seen in Fig. 6(c).

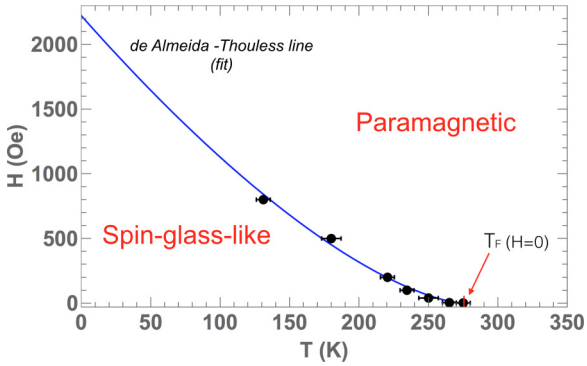

FIG. 7. (Color online) The irreversible behavior is characterized by an H-T magnetic phase diagram showing an AT line, which separates the spin-glass-like state from the paramagnetic phase. The AT line is determined experimentally (black dots) using the data from the ZFC and FC measurements and calculated (blue line) using a zero-field freezing temperature of 275 K and a zero-temperature critical field of 2220 Oe in Eq. (6).

The resulting phase diagram in the H-T plane is shown in Fig. 7. The AT line normally represents the critical points for transition between an ergodic phase to a nonergodic phase, with no change in the symmetry [44–46]. Therefore, the AT line separates a spin-glass phase (nonergodic) from a paramagnetic phase (ergodic). Thus, one can see that, for the almost entire range of temperature from 0 K to T_C, the FM order of Mn_5Ge_3 overlaps with the stability domain of the spin-glass-like state, provided that the magnetic field is low enough. The Curie temperature is barely 20 K above the zero-field spin-glass transition temperature. This means there is a small range of temperature (between 275 and 294 K), for which the system behaves as a pure ferromagnet. This observation explains why in the vicinity of the Curie temperature, the magnetization hysteresis curve [see Fig. 2(a)] has a high remanence ratio, due to the high intrinsic in-plane anisotropy of the ferromagnetic phase in the thin film. Below $T_F(H=0) \simeq 275$ K, the hysteresis has a weaker remanence ratio [see Fig. 2(b)] due to the influence of a spin-glass-like state.

The previous results are actually not sufficient to claim that the Mn_5Ge_3 thin film undergoes a true spin-glass phase

transition. We can only claim that the behavior under the AT line is spin-glass-like. In order to determine whether an actual spin-glass phase transition takes place or not, it is necessary to measure the nonlinear susceptibility of the sample. Unfortunately, the magnitude of the linear susceptibility is already quite small, and because of the fact that the nonlinear contribution is at least one order of magnitude smaller, the nonlinear susceptibility measurement is difficult in the present case.

C. Possible origin of the spin-glass-like behavior

Since the coexistence of the frustration and randomness is required for the spin-glass behavior, observation of the magnetic irreversibility in the single crystalline, i.e., ordered Mn_5Ge_3, is somewhat puzzling. However, as mentioned earlier, Mn_5Ge_3 on Ge(111) has a "ferromagnetically dead" layer at the Mn_5Ge_3/Ge interface [18]. Therefore, it is possible that this "dead layer," resulting most likely from the intermixing between the ferromagnetic Mn_5Ge_3 and Ge and from the lattice mismatch between the two materials, can possess the disorder needed for the spin-glass-like behavior, especially since there has been a previous report that disordered Mn-Ge compounds could demonstrate the spin-glass behavior [49]. Thus, the hypothesis here is that the system is actually made of two magnetic layers, one of which is ferromagnetic and the other is spin glass. The overall glassy behavior of the sample is due to the interaction between the ferromagnetic Mn_5Ge_3 with the thin spin-glass-like region. By using samples grown in the same conditions as samples A and C with different thicknesses, we estimated the thickness of the "ferromagnetically dead" layer to be 1.9 ± 0.2 nm. The presence of the sudden increase in magnetization at 65 K for decreasing temperature in Fig. 3 can be seen as the consequence of the exchange coupling at the interface between the spin-glass region and the FM phase. The kink in the FC magnetization happens at a temperature that is relatively low compared to the zero-field spin-glass-like transition temperature. In previous reports, a noticeable feature of many metallic spin glasses (such as CuMn, AgMn, AuFe, Ni-Mn alloys) was the occurrence of unidirectional anisotropy [50–55] for $T \ll T_F$ (typically $T < T_F/3$, see Ref. [50]). In our case, the presence of a low-temperature unidirectional anisotropy can create an additional easy axis in the FM phase along the applied field during the FC process, thus increasing the magnetization below a certain temperature. A widely used criterion for evaluating the presence of a unidirectional anisotropy is the presence of an exchange bias field. However, in our case the spin-glass region may be too small to induce a measurable exchange bias field in the FM region. Such a low-temperature kink in the FC magnetization has also been observed below the spin-glass transition temperature in ferromagnetic systems that share interfaces with spin glasses, such as $\gamma-Fe_2O_3$, $La_{2/3}Sr_{1/3}MnO_3$, and $La_{0.7}Ca_{0.3}MnO_3$, and the behavior was attributed to the effect of spin-glass interfaces [7,9,10,56]. In Refs. [7,9,10], the magnetization kink was also the onset of exchange bias. In addition, temperature-dependent magnetization curves measured at fields as high as 10^4 Oe have no kink at 65 K. The kink in the FC magnetization is visible only below the AT line, which confirms its relationship to the spin-glass-like state.

The irreversible behavior of the thermal magnetization in the Mn_5Ge_3/Ge(111) heterostructure can be explained as follows. Under the ZFC condition, the directions of the spins in the spin-glass region are randomly oriented and thus the spins in the spin-glass region are randomly coupled with the spins of the FM region near the interface. Such random coupling makes the motion of the domain walls unfavorable. As a result, for decreasing temperature the ZFC magnetization becomes small (Fig. 3) and the coercive field becomes large [Fig. 2(b)]. Under the FC condition, the directions of the spins in the spin-glass region tend to align more with the external field, so the randomness in the magnetic coupling between the FM and the spin-glass regions is diminished. Consequently, the magnetic domains move more easily, allowing the FC magnetization to become large. However, the coercivity remains large because the directions of the spins in the spin-glass region are still random, even under the FC condition.

Since the scaling laws showed that the spin-glass-like region at the Mn_5Ge_3/Ge interface behaves like a canonical spin glass, it is reasonable to assume that this region is made of Mn atoms embedded in a Ge-rich phase, thus making a case comparable to the above-mentioned spin glasses. Considering that the interactions between Mn atoms in the spin-glass region are mediated by conduction electrons, the Ruderman-Kittel-Kasuya-Yoshida (RKKY) model [51,52,57,58] allows to evaluate the freezing temperature as follows $T_F \sim V_0 S^2 d^{-3}$ [57], where V_0 is the RKKY coupling constant, S is the spin of Mn, and d is the average distance between Mn atoms. Consequently, the high spin-glass transition temperature in our system can be interpreted as the fact that the average distance between Mn atoms in the spin-glass region is relatively small.

Assuming that the "dead layer" or spin-glass-like layer originates from the interdiffusion at the interface during the solid phase epitaxy, it would be natural to consider that its properties are dependent on the thin film growth conditions. The magnetic properties of samples B and C (described in Table I) are discussed in the following section. Although the structural characterizations of samples B and C give the same results as those for sample A, the annealing temperature employed for the solid phase epitaxy and the film thickness have an influence on the thermal irreversibility of the magnetization in Mn_5Ge_3 on Ge(111).

IV. INFLUENCE OF THE GROWTH CONDITIONS ON THE THERMAL IRREVERSIBILITY

A. Influence of the annealing temperature for the solid phase epitaxy

Sample B was fabricated using a higher annealing temperature than that for sample A. The ZFC and FC magnetizations behavior of sample B [Fig. 8(a)] is substantially different from the ones shown for sample A in Fig. 3. The temperature dependence of the real part of the susceptibility [Fig. 8(b)] has distinct features from the case of sample A; the Curie point is lower than that of sample A by four degrees ($T_C \simeq 290$ K).

From the ZFC and FC curves, one can see that the onset of irreversibility, marked by T_{irr}, occurs at a temperature higher

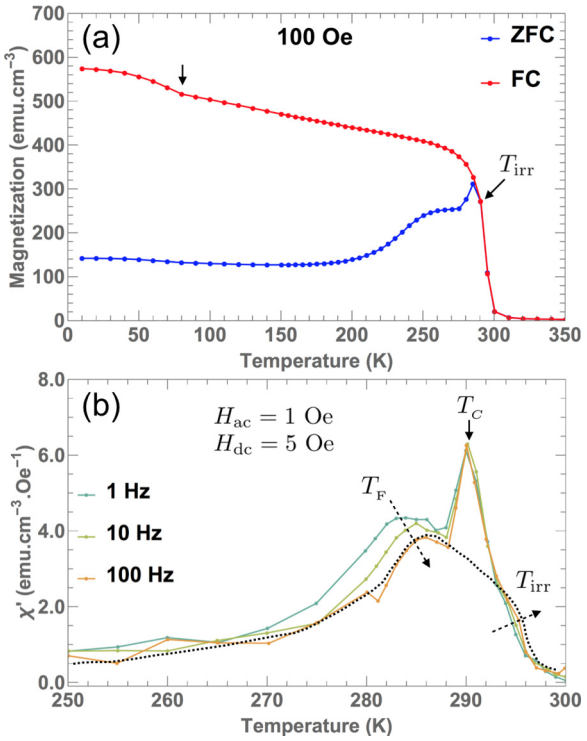

FIG. 8. (Color online) (a) ZFC and FC curves measured at a dc field of 100 Oe for sample B. (b) Frequency dependence of the in-phase component of the ac susceptibility, using a driving amplitude of 1 Oe and a bias dc field of 5 Oe. The Curie point is about 290 K and the peak corresponding to the irreversible behavior seems to overlap with the frequency-independent peak, as suggested by the eye-guiding dashed curve in (b). The sudden increase in FC magnetization is marked by an arrow at 80 K.

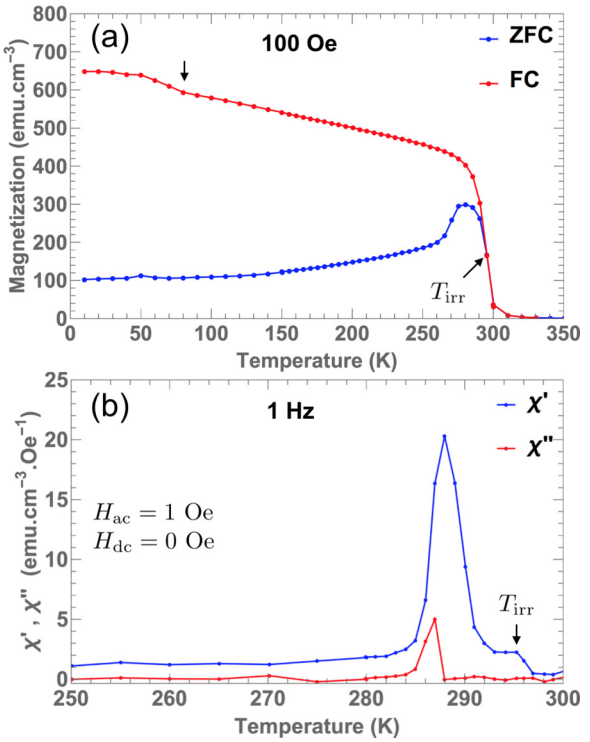

FIG. 9. (Color online) (a) ZFC and FC curves measured at a dc field of 100 Oe for sample C. (b) Real and imaginary parts of the ac susceptibility measured without bias dc field. The Curie point is about 288 K, which is slightly lower than that of sample B. The irreversibility temperature is higher than the Curie point $T_{irr} \simeq 295$ K. The sudden increase in FC magnetization is marked by an arrow at 80 K.

than the Curie point. This is a consequence of the higher growth temperature, which broadens the spin-glass transition temperature region, as evidenced by the observation of a frequency dependence of the real part of the susceptibility both below and above T_c in Fig. 8(b). Thus, a small portion of the spin-glass region has a transition temperature at around T_{irr} but a large portion of the spin-glass region has its transition at around T_F. As for sample A, the difference between the ZFC and FC magnetizations is due to the interaction between the spin-glass region and the FM region. The weak irreversibility just below T_{irr} in the ZFC and FC curves may be attributed to the sole contribution of the spin-glass region, which has a smaller size compared to the overall size of the sample. The difference between the FC and ZFC magnetizations becomes significant when Mn_5Ge_3 enters the FM phase. From the data in Fig. 8(b), we obtain $\delta T_F \simeq 0.005$, which is in agreement with sample A. As for sample A, the low-temperature kink in the FC magnetization is visible in sample B, accounting for the same effect discussed above. However, the onset of the kink in sample B is at about 80 K, which is higher than that of sample A.

B. Influence of the thickness

Sample C is grown in the same conditions as sample A but its thickness is larger. Similar to sample B, the spin-glass region in sample C shows the transition from PM to spin-glass above the Curie temperature of the FM phase [see Fig. 9(a)]. This is confirmed by the relative positions of the two maxima in the real part of the susceptibility [Fig. 9(b)], from which we estimate $T_c \simeq 288$ K and $T_{irr} = 295$ K. The position of the maximum of χ'' shows that the most visible relaxation process occurs just below T_c, while no maximum of comparable magnitude is present in the vicinity of T_{irr}. So, the main relaxation process occurs in the FM state. This behavior is similar to that of sample B. A sudden increase of FC magnetization is observed at 80 K as well. The main feature of sample C is the larger difference between the FC and ZFC magnetizations at low temperature, compared to the case of sample A. This is due to the fact that the ferromagnetic volume in sample C is larger than that in sample A, but the spin-glass volume around the interface is kept the same in both cases.

Despite demonstrating the quantitative variation in the magnetic properties depending on the growth conditions, samples A, B, and C share common traits, which are the presence of the slow magnetization relaxation close to the Curie point and the low-temperature kink in the FC magnetization. The susceptibility measurements for samples B and C imply that the spin-glass region alone is too small to induce a visible maximum in χ'', however, for decreasing temperature, a clear slow magnetization dynamics is obtained when the FM state is reached, thus evidencing the interaction between the two regions. In sample A, since the spin-glass transition occurs below the Curie point,

the slow dynamics is obtained at the transition point, i.e., T_{irr} and T_F are identical for sample A. The origin of the spin-glass-like behavior itself is extrinsic to the ferromagnetic Mn_5Ge_3 thin film. However, the spin-glass-like nature of the interface layer significantly affects the temperature-dependent behavior of the magnetization of the Mn_5Ge_3/Ge(111) heterostructure. It was reported in previous literatures [18,59,60] that the remanence ratio decreased with increasing thickness for both in-plane and perpendicular magnetizations. Since the easy axis of the bulk material is along the hexagonal *c* axis, one would expect larger perpendicular remanences for larger thicknesses of thin films. The interfacial glassy behavior shown in this work is very likely to explain the great differences between the bulk material and Mn_5Ge_3 films on Ge(111) at higher thicknesses.

V. SUMMARY AND CONCLUSION

Mn_5Ge_3 epitaxial thin films on Ge(111) do not show a simple ferromagnetic ordering expected for the bulk Mn_5Ge_3. Films grown at 150 °C via solid phase epitaxy undergo a transition to a spin-blocked state, for which the transition temperature at zero field is relatively close to the Curie point. The analysis of the ac susceptibility indicates that the spin-blocked state is spin-glass-like. Such transition to the glassy state explains the very different shapes of the magnetization cycles in the vicinity of T_C from the ones at low temperature. This spin-glass-like behavior is attributed to the presence of a "ferromagnetically dead layer" or more directly the spin-glass-like layer at the Mn_5Ge_3/Ge interface that is formed during the solid phase epitaxy process. Thus, the Mn_5Ge_3 film is separated into two layers, one of which is ferromagnetic. The spin-glass-like nature attributed to the interface-side layer explains the presence of the thermal irreversibility in the magnetization due to the frustrated interactions with the ferromagnetic Mn_5Ge_3. The spin-glass-like nature for the "ferromagnetically dead layer" is supported by the scaling laws. The fact that the magnetization irreversibility in Mn_5Ge_3 thin films is affected by the growth temperature and the thickness of the FM region, while the structure of the Mn_5Ge_3 layer remains the same, supports the hypothesis on a variation of magnetic properties due to the Mn_5Ge_3/Ge interface rather than the FM region. At higher growth temperature (200 °C), the Curie point becomes slightly lower and the irreversibility occurs above T_C. For a larger thickness (33 nm), the irreversibility also occurs above T_C, but the FC and ZFC magnetizations show the larger difference at low temperatures. Despite the FM behavior at high temperature and the glassy state at low temperature, the system is much different from a reentrant spin glass because of the extrinsic character of the spin-glass state.

ACKNOWLEDGMENTS

We appreciate R. Kiga for his technical support. This work was supported in part by the Grant-in-Aid for Scientific Research by MEXT, in part by NanoQuine, in part by JSPS Core-to-Core Program, in part by the Cooperative Research Project of the Research Institute of Electrical Communication, Tohoku University, and in part by the Collaborative Research Project of the Materials and Structures Laboratory, Tokyo Institute of Technology.

[1] K. Binder and A. P. Young, Rev. Mod. Phys. **58**, 801 (1986).
[2] J. S. Kouvel, J. Phys. Chem. Solids **21**, 57 (1961).
[3] M. Ali, P. Adie, C. H. Marrows, D. Greig, B. J. Hickey, and R. L. Stamps, Nat. Mater. **6**, 70 (2007).
[4] F. T. Yuan, J. K. Lin, Y. D. Yao, and S. F. Lee, Appl. Phys. Lett. **96**, 162502 (2010).
[5] R. Iguchi, K. Ando, E. Saitoh, and T. Sato, J. Phys.: Conf. Ser. **266**, 012089 (2011).
[6] J. F. Ding, O. I. Lebedev, S. Turner, Y. F. Tian, W. J. Hu, J. W. Seo, C. Panagopoulos, W. Prellier, G. Van Tendeloo, and T. Wu, Phys. Rev. B **87**, 054428 (2013).
[7] T. Zhu, B. G. Shen, J. R. Sun, H. W. Zhao, and W. S. Zhan, Appl. Phys. Lett. **78**, 3863 (2001).
[8] R. H. Kodama, A. E. Berkowitz, E. J. McNiff Jr., and S. Foner, Phys. Rev. Lett. **77**, 394 (1996).
[9] B. Martínez, X. Obradors, Ll. Balcells, A. Rouanet, and C. Monty, Phys. Rev. Lett. **80**, 181 (1998).
[10] S. B. Xi, W. J. Lu, H. Y. Wu, P. Tong, and Y. P. Sun, J. Appl. Phys. **112**, 123903 (2012).
[11] C. Zeng, S. C. Erwin, L. C. Feldman, A. P. Li, R. Jin, Y. Song, J. R. Thompson, and H. H. Weitering, Appl. Phys. Lett. **83**, 5002 (2003).
[12] C. Zeng, W. Zhu, S. C. Erwin, Z. Zhang, and H. H. Weitering, Phys. Rev. B **70**, 205340 (2004).
[13] L. Sangaletti, D. Ghidoni, S. Pagliara, A. Goldoni, A. Morgante, L. Floreano, A. Cossaro, M. C. Mozzati, and C. B. Azzoni, Phys. Rev. B **72**, 035434 (2005).
[14] L. Sangaletti, E. Magnano, F. Bondino, C. Cepek, A. Sepe, and A. Goldoni, Phys. Rev. B **75**, 153311 (2007).
[15] S. Olive-Mendez, A. Spiesser, L. A. Michez, V. Le Thanh, A. Glachant, J. Derrien, T. Devillers, A. Barski, and M. Jamet, Thin Solid Films **517**, 191 (2008).
[16] J. Hirvonen Grytzelius, H. M. Zhang, and L. S. O. Johansson, Phys. Rev. B **86**, 125313 (2012).
[17] S. Picozzi, A. Continenza, and A. J. Freeman, Phys. Rev. B **70**, 235205 (2004).
[18] A. Spiesser, F. Virot, L. A. Michez, R. Hayn, S. Bertaina, L. Favre, M. Petit, and V. Le Thanh, Phys. Rev. B **86**, 035211 (2012).
[19] P. De Padova, J. M. Mariot, L. Favre, I. Berbezier, B. Olivieri, P. Perfetti, C. Quaresima, C. Ottaviani, A. Taleb-Ibrahimi, P. Le Fèvre, F. Bertran, O. Heckmann, M. C. Richter, W. Ndiaye, F. D'Orazio, F. Lucari, C. M. Cacho, and K. Hricovini, Surf. Sci. **605**, 638 (2011).
[20] M. Sawicki, W. Stefanowicz, and A. Ney, Semicond. Sci. Technol. **26**, 064006 (2011).
[21] A. Truong, A. O. Watanabe, T. Sekiguchi, P. A. Mortemousque, T. Sato, K. Ando, and K. M. Itoh, Phys. Rev. B. **90**, 224415 (2014).

[22] E. Callen, Y. J. Liu, and J. R. Cullen, Phys. Rev. B **16**, 263 (1977).
[23] S. Chikazumi, *Physics of Magnetism* (Wiley, New York, 1964), p. 247.
[24] I. Maartense and G. Williams, J. Phys. F: Met. Phys. **6**, L121 (1976).
[25] F. H. Salas and M. Mirabal-García, Phys. Rev. B **41**, 10859 (1990).
[26] P. Nordblad, P. Svedlindh, L. Lundgren, and L. Sandlund, Phys. Rev. B **33**, 645(R) (1986).
[27] M. A. Continentino and A. P. Malozemoff, Phys. Rev. B **33**, 3591(R) (1986).
[28] R. V. Chamberlin, G. Mozurkewich, and R. Orbach, Phys. Rev. Lett. **52**, 867 (1984).
[29] S. D. Tiwari and K. P. Rajeev, Phys. Rev. B **72**, 104433 (2005).
[30] D. X. Li, S. Nimori, Y. Shiokawa, Y. Haga, E. Yamamoto, and Y. Onuki, Phys. Rev. B **68**, 012413 (2003).
[31] D. X. Li, S. Nimori, Y. Shiokawa, Y. Haga, E. Yamamoto, and Y. Onuki, Phys. Rev. B **68**, 172405 (2003).
[32] C. N. Guy, J. Phys. F: Met. Phys. **8**, 1309 (1978).
[33] Y. T. Wang, H. Y. Bai, M. X. Pan, D. Q. Zhao, and W. H. Wang, Phys. Rev. B **74**, 064422 (2006).
[34] V. K. Anand, D. T. Adroja, and A. D. Hillier, Phys. Rev. B **85**, 014418 (2012).
[35] J. A. Mydosh, *Spin Glass: An Experimental Introduction* (Taylor and Francis, London, 1993).
[36] Z. Fu, Y. Zheng, Y. Xiao, S. Bedanta, A. Senyshyn, G. G. Simeoni, Y. Su, U. Rücker, and P. Kögerler, and T. Brückel. Phys. Rev. B **87**, 214406 (2013).
[37] L. Ma, W. H. Wang, J. B. Lu, J. Q. Li, C. M. Zhen, D. L. Hou, and G. H. Wu, Appl. Phys. Lett. **99**, 182507 (2011).
[38] P. C. Hohenberg and B. I. Halperin, Rev. Mod. Phys. **49**, 435 (1977).
[39] J. Souletie and J. L. Tholence, Phys. Rev. B **32**, 516 (1985).
[40] S. Shtrikman and E. P. Wohlfarth, Phys. Lett. A **85**, 467 (1981).
[41] C. A. Cardoso, F. M. Araujo-Moreira, V. P. S. Awana, E. Takayama-Muromachi, O. F. de Lima, H. Yamauchi, and M. Karppinen, Phys. Rev. B **67**, 020407(R) (2003).
[42] J. L. Tholence, Solid State Commun. **35**, 113 (1980).
[43] H. Aruga Katori and A. Ito, J. Phys. Soc. Jpn. **63**, 3122 (1994).
[44] A. P. Young and H. G. Katzgraber, Phys. Rev. Lett. **93**, 207203 (2004).
[45] H. G. Katzgraber and A. P. Young, Phys. Rev. B **72**, 184416 (2005).
[46] H. G. Katzgraber, D. Larson, and A. P. Young, Phys. Rev. Lett. **102**, 177205 (2009).
[47] J. R. L. de Almeida and D. J. Thouless, J. Phys. A: Math. Gen. **11**, 5 (1978).
[48] M. Gruyters, Phys. Rev. Lett. **95**, 077204 (2005).
[49] J. J. Hauser, J. Magn. Magn. Mater. **15-18**, 1387 (1980).
[50] F. Hippert and H. Alloul, J. Phys. (Paris) **43**, 691 (1982).
[51] J. B. Staunton, B. L. Gyorffy, J. Poulter, and P. Strange, J. Phys.: Condens. Matter **1**, 5157 (1989).
[52] P. M. Levy, C. Morgan-Pond, and A. Fert, J. Appl. Phys. **53**, 2168 (1982).
[53] T. Sato, Phys. Rev. B **41**, 2550 (1990).
[54] Y. Öner and H. Sari, Phys. Rev. B **49**, 5999 (1994).
[55] J. S. Kouvel, W. Abdul-Razzaq, and Kh. Ziq, Phys. Rev. B **35**, 1768 (1987).
[56] P. Dey, T. K. Nath, P. K. Manna, and S. M. Yusuf, J. Appl. Phys. **104**, 103907 (2008).
[57] S. N. Lyakhimets, IEEE Trans. Magn. **30**, 840 (1994).
[58] P. M. Levy and A. Fert, Phys. Rev. B **23**, 4667 (1981).
[59] A. Spiesser, S. F. Olive-Mendez, M. T. Dau, L. A. Michez, A. Watanabe, V. Le Thanh, A. Glachant, J. Derrien, A. Barski, and M. Jamet, Thin Solid Films **518**, S113 (2010).
[60] V. Le Thanh, A. Spiesser, M. T. Dau, S. F. Olive-Mendez, L. A. Michez, and M. Petit, Adv. Nat. Sci.: Nanosci. Nanotechnol. **4**, 043002 (2013).